Liquid Crystals
Publication details, including instructions for authors and subscription information:
http://www.informaworld.com/smpp/title~content=t713926090

New method for measuring polar anchoring energy of nematic liquid crystals

Anatoli Murauski[a]; Vladimir Chigrinov[a]; Hoi-Sing Kwok[a]
[a] ECE Department, Hong Kong University of Science & Technology, Clear Water Bay, Kowloon, Hong Kong

To cite this Article Murauski, Anatoli , Chigrinov, Vladimir and Kwok, Hoi-Sing(2009) 'New method for measuring polar anchoring energy of nematic liquid crystals', Liquid Crystals, 36: 8, 779 — 786
To link to this Article: DOI: 10.1080/02678290903047136
URL: http://dx.doi.org/10.1080/02678290903047136

Liquid Crystals,
Vol. 36, No. 8, August 2009, 779–786

New method for measuring polar anchoring energy of nematic liquid crystals

Anatoli Murauski*, Vladimir Chigrinov and Hoi-Sing Kwok

ECE Department, Hong Kong University of Science & Technology, Clear Water Bay, Kowloon, Hong Kong

(Received 6 May 2009; final form 15 May 2009)

A new method for measuring a polar anchoring energy of nematic liquid crystals (LCs) is proposed. A variation of LC tilt angle on the surface with an applied electrical field was determined by a reflective method. The twisted LC cell configuration was selected to compensate a contribution of the induced birefringence in the reflective spectra. The electrical field controlled reflectance was used to analyse the potential form of the polar anchoring energy and to define the anchoring strength. The proposed method is applicable for 2–5 μm thick LC cells.

Keywords: anchoring energy; liquid crystal; reflective measurements; surface tilt angle

1. Introduction

Liquid crystal (LC) anchoring energy is an important parameter of LC cells which defines the basic characteristics of LC electro-optic response, such as controlling voltage and response time (*1*). The dependence of an anchoring energy from the deviation of LC pretilt angle from an equilibrium state has been widely discussed in the literature (*2–4*). The Rapini–Papoular relation for anchoring energy was usually used for the purpose (*3*). However, some authors claim that Rapini–Papoular approximation is not a universal approach and there exist several cases where the approach is not correct (*5, 6*). At the same time, we should note that most of the LC anchoring energy measurements methods are based on the Rapini–Papoular formula (*3*).

Usually LC anchoring energy is found from the dependence of the LC bulk parameters such as a retardation or capacity versus applied electric or magnetic field for LC cells with a large cell gap (*7–16*). The most effective method is a high voltage technique proposed by Yokoyama and van Sprang (*10*). A modification of this method is the RV technique developed by Kent University (*11, 12*). The polar anchoring energy can also be found from electrical measurement by a capacitance method (*13–15*). The method to evaluate a polar (or zenithal) LC anchoring energy proposed by Vilfan *et al.* uses the measurements of relaxation time of LC director fluctuations in a homogeneously aligned cell as a function of LC cell thickness (*16, 17*).

The disadvantage of the 'bulk' methods is a small contribution of the LC anchoring effect, so the measurements of the LC anchoring energy become inefficient. To minimise the volume effects when measuring the anchoring energy we explored the compensation principle. The principle states that all the effects not related to the interaction of LC with the surface are automatically excluded and do not influence the measurements data. The technique was successfully realised in two channel capacity methods (*14*). In this case the vertical aligned (VA) LC cell was used as a reference channel in a measurement set up to increase a precision of the electrical method (*14*). We propose another compensation method for optical measurements, shown in this paper. We used a high voltage deformed twist LC cell, where the volume birefringence is totally compensated, as the cell can be presented by two birefringence plates with mutually orthogonal directions of their optical axes. We measured the anisotropy of reflectivity on the boundary isotropic–anisotropic materials (liquid crystal–alignment material). The compensation of LC birefringence in the 90° twisted cell strongly minimises the effect of LC birefringence in volume. The reflective coefficient at the isotropic–anisotropic boundary in LC cell is determined by the LC tilt angle nearest to the surface. The LC amplitude reflections can be precisely measured for any applied voltage. This dependence can be used for the evaluation of a LC polar anchoring energy.

2. Theoretical background

The distribution of a LC director inside the cell is determined by LC elastic and dielectric constants and by the value of the electrical field applied to the LC cell. This distribution can be calculated for any pretilt angle on the boundary in the case of strong anchoring interaction between LC and the alignment surface. In the case of semi-infinite configuration for LC and infinite anchoring energy we can write simple analytical expressions for the LC director distribution. Such

*Corresponding author. Email: eemuraan@ust.hk

ISSN 0267-8292 print/ISSN 1366-5855 online

DOI: 10.1080/02678290903047136
http://www.informaworld.com

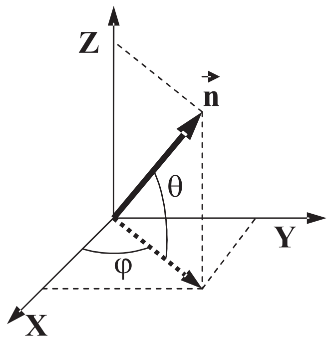

Figure 1. Polar θ and azimuthal φ angles of LC director. XY is the substrate plane.

conditions are realised when a high electrical field is applied to the LC cell and the tilt angle of LC molecules at the centre of the LC cell is equal to 90°. Figure 1 shows the corresponding LC director orientation angles θ and φ with respect to the substrate plane XY. The LC optical properties can be easily calculated if the director distribution is known.

For sufficiently high voltage ($V > 6V_{th}$) the director angle at the centre of the LC cell becomes almost equal to $\theta_m = \pi/2$. Thus the LC cell can be considered to consist of two independent parts: two highly distorted regions with fast transition from the tilt angle on the boundary to vertical alignment in the centre of the cell. The distribution of the LC polar angle $\theta(z)$ for the applied voltage V can be written as (*11*)

$$z = \frac{dV_{th}}{\pi V} \int_{\theta_S}^{\theta} \sqrt{\frac{(1+\gamma \sin^2 x)(1-a\cos^2 x)}{1-\sin^2 x}} dx, \qquad (1)$$

where $\gamma = (K_{33} - K_{11})/K_{11}$, $a = \Delta\varepsilon/\varepsilon_{||}$, $\Delta\varepsilon = (\varepsilon_{||} - \varepsilon_{\perp})$, $V_{th} = \pi\sqrt{K_{11}/\varepsilon_0 \Delta\varepsilon}$.

If the liquid crystal is not chiral then the variation of the LC azimuthal angle φ will concentrate at the centre of the cell and will not change in each highly distorted region of the LC cell. In a 90° twisted LC cell the boundary parts with highly distorted orientation are orientated orthogonal to each other. The distribution inside every part is the same as in a non-twisted (splay-bend) LC cell (*1*). This property produces unique optical qualities of LC twist cell: the phase difference between two independent polarisations of the transmitted light is zero. This unique property of a 90° twisted LC cell enables the realisation of a compensation principle and the avoidance of the bulk birefringence effect in this cell. This means that for sufficiently large voltage ($V > 6V_{th}$) the bulk birefringence of the LC twist cell will disappear (Figure 2).

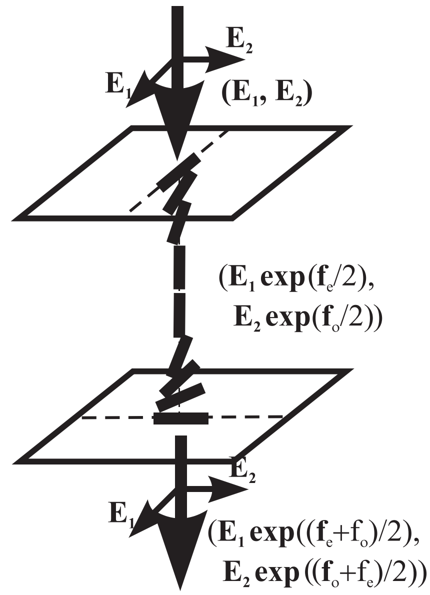

Figure 2. LC director configuration in 90° twist cell, when high voltage is applied to the twisted LC cell ($V > 6V_{th}$).

Consequently, the reflection of a 90° twisted LC cell will be defined by the interference of two light waves reflected from two boundaries of LC with the substrates.

2.1 Reflection coefficient for boundary isotropic–isotropic medium

Let us consider the reflection from the isotropic–isotropic medium boundary in an LC cell. A linearly polarised light is incident normally to an LC cell, and the angle between the polarisation direction and extraordinary axis of the LC layer is η. Let us consider first only one boundary which reflects light. This boundary is the interface between two media with refractive indexes n_1 and n_2. Let the amplitude of the input polarised light be A_{in} and the amplitude of the output reflected light after the analyser A_{out}. Let the angle between the polariser and analyser be ϕ. Figure 3 shows the optical scheme.

The two waves propagate in an anisotropic LC medium: ordinary E_o (refractive index n_o) and extraordinary E_e (refractive index n_e),

$$\begin{aligned} E_e &= A_{in}\cos(\eta)\, e^{i2\pi\frac{n_e d}{\lambda}}, \\ E_o &= A_{in}\sin(\eta)\, e^{i2\pi\frac{n_o d}{\lambda}}. \end{aligned} \qquad (2)$$

The reflection coefficient for the boundary isotropic–isotropic medium for both waves E_o and E_e is the same and the amplitudes of the reflected waves F_o and F_e:

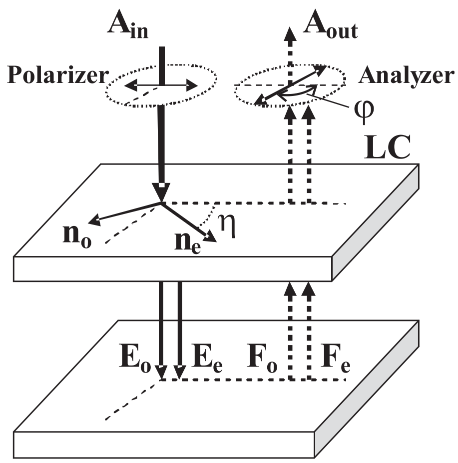

Figure 3. Reflection of the polarized light from the isotropic–isotropic boundary.

$$F_e = r_{is} \cdot A_{in} \cos(\eta)\, e^{i2\pi \frac{n_e d}{\lambda}},$$
$$F_o = r_{is} \cdot A_{in} \sin(\eta)\, e^{i2\pi \frac{n_o d}{\lambda}}, \tag{3}$$

where $r_{is} = \frac{n_1 - n_2}{n_1 + n_2}$, n_1 and n_2 are refractive indexes of the two isotropic media.

The light goes back through an anisotropic LC layer, which doubles the phase retardation for every wave, and finally passes through the analyser (Figure 3). In this case we have

$$A_{out} = r_{is} A_{in} \left(\cos(\eta)\cos(\eta + \phi)\, e^{i4\pi \frac{n_e d}{\lambda}} + \sin(\eta)\sin(\eta + \phi)\, e^{i4\pi \frac{n_o d}{\lambda}} \right). \tag{4}$$

If the analyser is crossed with the polariser we can get from Equation (4)

$$A_{out} = r_{is} A_{in} \sin(2\eta)\, \sin\left(2\pi \frac{\Delta n\, d}{\lambda}\right) \cdot i \cdot e^{i2\pi \frac{(n_e + n_o)\, d}{\lambda}}. \tag{5}$$

Equation (5) states that, in the case of crossed analyser and polariser, the amplitude of the output light is zero if the overall birefringence Δn of all the isotropic layers between the polariser and analyser from one side and reflective boundary from the other side is zero.

2.2 Reflection coefficient for the boundary liquid crystal–isotropic medium

The light propagation in the LC layer can be described using two orthogonal waves: an ordinary and an extraordinary. The reflection from the LC boundary for an ordinary wave $r^o_{an} = R_o$ is a simple Fresnel reflection from the boundary between two isotropic media but for the extraordinary wave r^e_{an} it is roughly a sum of the two reflective waves (*18*). One wave is the reflection from the boundary (Fresnel reflection R_e) and the other is the reflection from the LC layer R_{LC}. The latter coefficient R_{LC} can be considerably different from R_e in the case of LC director deformation in the electrical field.

$$r^o_{an} = R_o = \frac{n^o_{LC} - n_{al}}{n^o_{LC} + n_{al}} \quad \text{and} \quad r^e_{an} = R_e + R_{LC}, \tag{6}$$

where $R_e = \frac{n^s_{LC} - n_{al}}{n^s_{LC} + n_{al}}$ is the reflection which does not depend on the bulk LC orientation and defines by LC extraordinary refractive index n^s_{LC} at the surface and R_{LC} is the part of the reflection coefficient which depends on the LC director distribution near the surface. An extraordinary refractive index n_e exhibits a non-zero gradient variation near the boundary related to the LC director deformation. The amplitude of the reflected wave can be found as a sum of all the waves reflected from the boundaries between the small sublayers with the thickness dz in the following form:

$$R_{LC} = \int_0^{d/2} \frac{1}{2n'_e} \frac{dn'_e}{dz} e^{if(z)} dz = \int_0^{d/2} \frac{1}{2n'_e} \frac{dn'_e}{d\theta} \frac{d\theta}{dz} e^{if(z)} dz, \tag{7}$$

where

$$f(z) = \frac{2\pi}{\lambda} \cdot 2 \int_0^z n'_e dz = \frac{4\pi}{\lambda} \int_{\theta_s}^{\theta} n'_e \frac{dz}{d\theta} d\theta$$

is the phase retardation of the extraordinary wave propagated in the LC layer, where $\theta\ (z = 0) = \theta_s$, and the integration is limited by the centre of the LC layer $z = d/2$, where the gradient $\frac{dn'_e}{dz}$ disappears in a sufficiently high electrical field applied to the LC layer. In this case LC orientation at the centre of the layer $\theta_m = \pi/2$, and we get from Equation (1)

$$\frac{dz}{d\theta} = \frac{dV_{th}}{\pi V} \sqrt{\frac{(1 + \gamma \sin^2\theta)(1 - a\cos^2\theta)}{1 - \sin^2\theta}}.$$

The effective extraordinary refractive index $n'_e(\theta)$ depends on the LC polar angle θ as

$$n'_e(\theta) = \frac{n_e n_o}{\sqrt{n_e^2 \sin^2\theta + n_o^2 \cos^2\theta}} = \frac{n_e}{\sqrt{1 + \beta^2 \sin^2\theta}}$$

and the value of the extraordinary refractive index on the boundary can be written as

$$n_{LC}^s = \frac{n_e}{\sqrt{1+\beta^2 \sin^2 \theta_s}}, \text{ where } \beta^2 = \frac{n_e^2 - n_o^2}{n_o^2}.$$

Equation (7) can be rewritten as

$$R_{LC} = \frac{1}{2}\int_{\theta_S}^{\pi/2} \frac{(n_e^2 - n_o^2)tg\theta}{n_o^2 + n_e^2 tg^2\theta} \exp\left(-i\frac{4n_e d}{\lambda}\frac{V_{th}}{V} \times \int_{\theta_S}^{\theta} \sqrt{\frac{(1+\gamma\sin^2 x)(1-a\cos^2 x)}{(1-\sin^2 x)(1+\beta^2\sin^2 x)}}dx\right)d\theta, \quad (8)$$

where θ_s is the angle of the LC director on the surface.

Equation (8) provides the amplitude of the reflection from the deformed LC layer for the extraordinary component of the incident light. Using the same procedure as in Section 2.1 and Equation (6) we can define the amplitude of the reflective light from the boundary LC–isotropic alignment layer as

$$A_{out} = A_{in}\left(r_{an}^e \cos(\eta)\cos(\eta+\phi) + r_{an}^o \sin(\eta)\sin(\eta+\phi)\right).$$

If the analyser is crossed with the polariser ($\phi = \pi/2$) and the retardation of the anisotropic layer is zero (Figure 3), the amplitude of the output light A_{out} can be written as (*18*)

$$A_{out} = \frac{1}{2}A_{in}(r_{an}^o - r_{an}^e)\sin 2\eta = -\frac{1}{2}A_{in}(R_e - R_o + R_{LC})\sin 2\eta. \quad (9)$$

The Fresnel's reflection contribution depends on the effective value of the LC refractive index on the boundary n_{LC}^s defined by the LC tilt angle on the boundary. The difference between the refractive index of the isotropic alignment material and LC ordinary refractive index provides a constant contribution to the reflective light, which is not dependent on the LC tilt angle on the surface. Thus, if the refractive index of the alignment material n_{al} is close to the ordinary refractive index of LC n_{LC}^o we have

$$R_e - R_o = \frac{n_{LC}^s - n_{al}}{n_{LC}^s + n_{al}} - \frac{n_{LC}^o - n_{al}}{n_{LC}^o + n_{al}} \approx \frac{n_{LC}^s - n_{LC}^o}{n_{LC}^s + n_{LC}^o}. \quad (10)$$

In this case the amplitude of the reflective light A_{out} (Equation (9)) is

$$A_{out} = -\frac{1}{2}A_{in} \cdot \sin 2\eta\left(\frac{n_{LC}^s - n_{LC}^o}{n_{LC}^s + n_{LC}^o} + R_{LC}\right). \quad (11)$$

The refractive index n_{LC}^s depends on the LC tilt angle on the boundary only, while the amplitude R_{LC} depends on the LC tilt angle on the boundary and on the voltage applied to LC layer.

The formula (Equation (11)) provides the amplitude for the reflection from one boundary of an LC cell. As an LC cell has two boundaries, the reflective light will be defined by the interference of the waves reflective from both boundaries of the LC layer. In the case of equal boundary conditions for an LC cell the simple formula can be obtained. A more interesting result comes for a 90° twist cell when a high voltage is applied. If the applied voltage is larger than $6V_{th}$, LC molecules at the centre of the cell are orientated vertical and the LC cell becomes separated into two parts with a symmetrical distribution of the LC director from the boundary to the cell centre. Both parts of the LC cell are not twisted but rotated on 90° with respect to each other. If the phase retardation of the light wave reflected from the top substrate is zero, then the phase retardation of the light reflected from the bottom boundary will be equal to $f_0 + f_e$, where $f_o = \frac{4\pi n_o d}{\lambda}$ is the phase retardation for the ordinary wave passed twice through the LC cell and f_e can be calculated similarly to Equation (7) and

$$f_e = f(d/2) = \frac{2\pi}{\lambda}\cdot 2\int_0^{d/2} n_e' dz.$$

The intensity of the reflected light Ir can be calculated as a result of the interference of the light waves reflected from the top and bottom LC cell boundary as

$$Ir = \left|A_{out} - A_{out}e^{i\frac{\varphi_o+\varphi_e}{2}}\right|^2.$$

Using Equation (11) we receive the intensity of the reflected light Ir for a 90° twist cell between crossed polarisers:

$$Ir = 2(A_{out})^2\sin^2\left(\frac{f_o+f_e}{4}\right) = \frac{1}{2}A_{in}^2\cdot\left(\frac{n_{LC}^s - n_{LC}^o}{n_{LC}^s + n_{LC}^o} - R_{LC}\right)^2\sin^2\left(\frac{f_o}{2}\right), \quad (12)$$

where we assume $f_e \approx f_o = 4\pi n_o d/\lambda$ and $\eta = \pi/4$.

Equation (12) is valid only when the input and output polarisers are crossed and a 90° twisted LC cell is orientated at $\eta = 45°$ to the polarisation of the input light. These special conditions exclude the contributions of all the reflection from the boundaries between isotropic mediums in an LC cell. Equation (12) can be presented in a normalised form, which does not include the amplitude of the input light A_{in}. The normalised value of the intensity becomes a function of the two parameters: one is LC tilt angle θ_s on the surface and the other is the reduced value of applied voltage $U' = \frac{V}{V_{th} d}$, while the other parameters of the LC cell remain the same:

$$Ir_{norm}(\theta_s, U') = \frac{Ir(\theta_s, U')}{Ir(0,0)} = \left(\frac{\frac{n^s_{LC} - n^o_{LC}}{n^s_{LC} + n^o_{LC}} - R_{LC}}{\left(\frac{n^s_{LC} - n^o_{LC}}{n^s_{LC} + n^o_{LC}} \right)_{\theta_s = 0}} \right)^2, \qquad (13)$$

where $n^s_{LC} = n^s_{LC}(\theta_s)$ and $R_{LC} = R_{LC}(\theta_s, U')$.

The dependence of the normalised amplitude reflection from the reduced voltage for different values of the LC director tilt angle on boundary liquid crystal–alignment layer is shown in Figure 4.

If an anchoring energy is finite, the tilt angle on the surface varies with the applied voltage. The dependence of the amplitude reflection is shown in Figure 4 by a dashed curve which crosses the reflectance curves calculated for a fixed tilt boundary angle, which corresponds to an infinite anchoring energy. If the dependence of the reflection amplitude is taken from experiment the point of intersection of the experimental curve with the lines calculated for infinite anchoring energy will correspond to the tilt angle on the boundary. This comes from the suggestion that if the boundary angles of the LC director are fixed, we may have only one possible distribution of the LC director in the bulk (*1*). By this way we can receive the dependence of the LC tilt angle on the surface.

The variation of the tilt angle on the surface is defined by the LC polar anchoring energy.

For a symmetrical LC cell with the thickness d the tilt angles on the boundary are

$$\theta_s = \theta(0) = \theta(d).$$

The voltage dependent torque-balance relation at the boundary condition is (*11*)

$$\frac{dF_s(\theta_s)}{d\theta_s} = \left(K_{11}\cos^2\theta + K_{33}\sin^2\theta\right)\frac{d\theta}{dz}\bigg|_{z=0}. \qquad (14)$$

For voltage $V > 6V_{th}$ Equation (14) can be written as

$$\frac{dF_s(\theta_s)}{d\theta_s} = \pi\frac{K_{11}}{d}\frac{\varepsilon^{av}(V)}{\varepsilon_{||}}\frac{V}{V_{th}}\frac{\sqrt{1+\gamma\sin^2\theta_s}}{\sqrt{1-a\cos^2\theta_s}}\cos\theta_s, \qquad (15)$$

where $\gamma = (K_{33} - K_{11})/K_{11}$, $a = \Delta\varepsilon/\varepsilon_{||}$, $V_{th} = \pi\sqrt{K_{11}/\varepsilon_0\Delta\varepsilon}$ is the threshold voltage, $\Delta\varepsilon = (\varepsilon_{||} - \varepsilon_{\perp})$, and $\varepsilon^{av}(V) = \varepsilon_{||}\left(1 - \alpha\frac{\Delta\varepsilon}{\varepsilon_{||}}\frac{V_{th}}{V}\right)$ is the average dielectric constant for the LC layer (*6*), $\alpha \approx 1$. For a sufficiently high voltage the LC director in a central part of the cell is orientated along the electrical field and can be estimated as

$$\varepsilon^{av}(V)\cdot V \approx \varepsilon_{||}\left(V - \frac{\Delta\varepsilon}{\varepsilon_{||}}V_{th}\right).$$

The dependence of an LC tilt angle on the boundary is completely determined by the anchoring

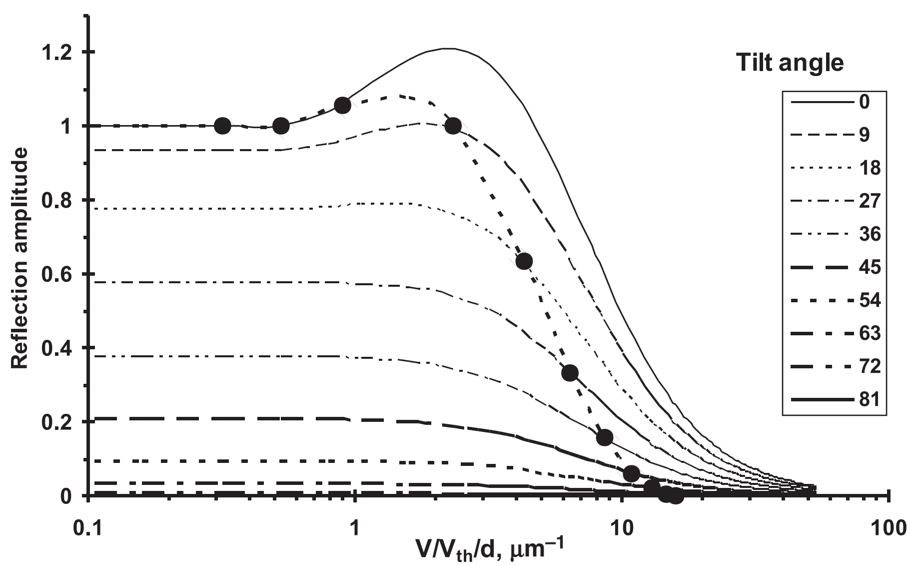

Figure 4. Calculated voltage dependence of the normalized reflection amplitude for various LC surface tilt angles and infinite LC polar anchoring energy. The experimental data are shown by black circles. The data for LC BN-104 were used in the calculations.

interaction between the LC and the alignment material. The simplest expression for the anchoring energy can be written in the form $F_s(\theta_s) = \frac{1}{2}W(\theta_s - \theta_0)^2$ for a small deviation, or Rapini–Papoular form (*4*) $F_s(\theta_s) = \frac{1}{2}W\sin^2(\theta_s - \theta_0)$ for larger deviations from the preferred LC director orientation on the boundary. For the small values of the LC tilt angle θ_s it is a linear function of the applied voltage:

$$\theta_s = \pi\frac{K_{11}}{W}\frac{V}{V_{th}\,d}\sqrt{\frac{\varepsilon_{||}}{\varepsilon_{\perp}}}. \tag{16}$$

For a sufficiently large pretilt angle, the anchoring coefficient W is not constant and varies with the LC tilt angle (*10*) as

$$W(\theta_s) = W_1 + (W_2 - W_1)\sin^2(\theta_s - \theta_0),$$

where the coefficient $W_2 - W_2$ characterises the second term in a power series of $\sin^2(\theta_s - \theta_0)$.

Figure 5 presents the dependence of the LC tilt angle at the boundary on voltage for the three above-mentioned LC anchoring potentials. All three potentials produce the same LC tilt angle dependence (tilt angle less than 20°) for a sufficiently small voltage. If we like to consider the effect of the anchoring voltage potential, we should allow for considerably larger LC tilt angles of up to 60° (Figure 5).

3. Experimental

The set-up for reflective measurements is shown in Figure 6. We used the polarised reflective microscope

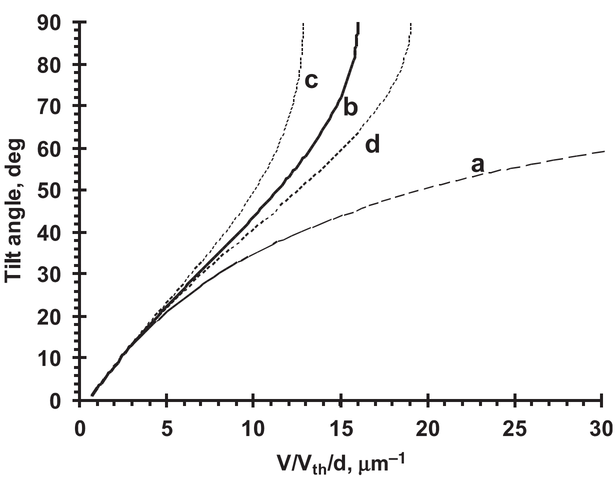

Figure 5. Dependence of the LC tilt angle at the boundary on applied voltage for various polar anchoring energy potential forms. (Square $F_s(\theta_s) = \frac{1}{2}W(\theta - \theta_0)^2$ (a); Rapini–Papoular $F_s(\theta_s) = \frac{1}{2}W\sin^2(\theta - \theta_0)$ (b); anisotropic Rapini–Papoular $W(\theta) = W_1 + (W_2 - W_1)\sin^2(\theta - \theta_0)$ $(W_2 - W_1 < 0$ (c) and $W_2 - W_1 > 0$ (d)).

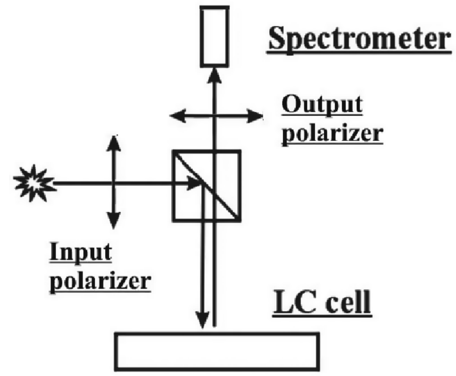

Figure 6. Optical scheme of the experimental set-up.

Olympus BX40. The high resolution spectrometer HD2000 from Ocean Optics was used for spectral measurements with a spectral resolution of 1.5 nm.

Several LC TN 90° cells with a cell gap of 2 μm were used in measurements. The glass substrates had patterned ITO electrodes with the LC cell overlapping an area of 5 × 5 mm^2. The alignment material was deposited on top of the ITO layer by a spin coating method. The thickness of the alignment layer was around 30 nm. We used three different alignment materials: (i) PIA-3744 from Chisso with a strong LC anchoring; (ii) photo aligned material SD-1 from DIC with medium values of polar anchoring energy (*14*); (iii) material B-15 with low polar anchoring energy (*19*). All the cells were filled with LC mixture BN-104 with a low threshold voltage and the following parameters at 25°C: elastic constants K_{11} = 7.5 pN, K_{22} = 5.6 pN, K_{33} = 12.2 pN, dielectric anisotropy $\Delta\varepsilon$ = 26.6, anisotropy of refractive index Δn = 0.163 for the wavelength λ = 650 nm. All the cells had a uniform 90° twist alignment without defects and disclination lines, which separates areas of LC with twist angle +90° and –90°.

The LC cell was placed under the polarised microscope and orientated at an angle of 45° with respect to the polarisation of the input light. The polarisation beam splitter transmitted to the spectrometer only one orthogonal component of the reflected light (the output polariser being orthogonal to the input polariser). When the applied voltage exceeds $V > 4V_{th}$ = 2.5 V the form of the reflection signal remains the same and only the amplitude of the signal is varied (Figure 7). The maximum reflectance amplitude dependence on voltage was measured at a wavelength close to 550 nm.

4. Results and discussion

We measured the dependence of the reflective signal amplitude versus applied voltage for all LC cells with

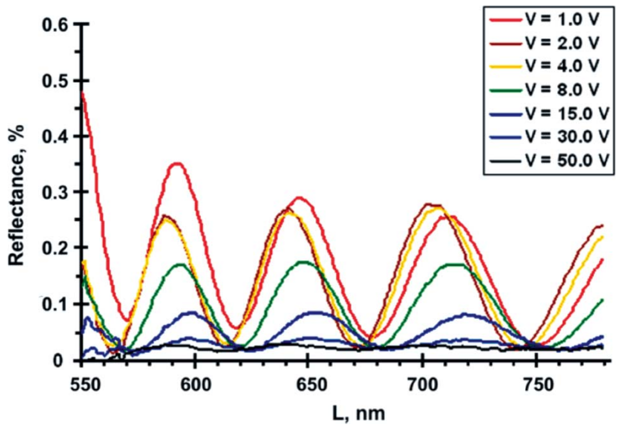

Figure 7. Reflection signal *versus* applied voltage. The LC cell thickness was 2 μm. LC mixture BN-104 and alignment material PIA-3744 were used.

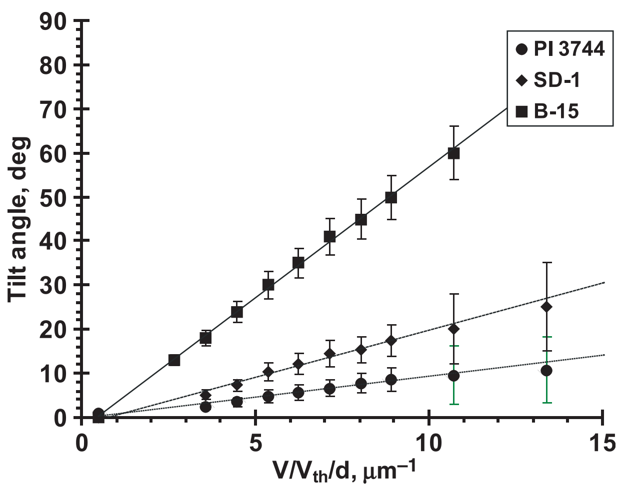

Figure 8. LC surface tilt angle *versus* applied voltage. The straight lines are linear approximations of the experimental data. The LC cell gap was 1.95 μm; LC material BN-104 was used.

different alignment films. We received the spectral dependence shown in Figure 8 for every LC cell.

We used the dependence of amplitude reflection maximum at a wavelength of 550 nm (about 18,000 cm^{-1}) to calculate the dependence of LC tilt angle on the applied voltage. The maximum voltage was limited by the parameter $\frac{V}{V_{th}d} < 20 \cdot \mu m^{-1}$. The amplitude of LC reflection in this case is small for any LC surface tilt angle thus significantly increasing the error in LC tilt angle determination. We used formula (12) for the calculations of the reflectance intensity and the procedure showed in Figure 4 to define LC pretilt angle on the surface. Figure 8 presents the results of our measurements.

We can see only small deviation from the equilibrium state for alignment materials with a strong LC anchoring energy when the tilt angle is less than 20°. In case of a high voltage ($V/V_{th}d > 30$ μm^{-1} for LC BN-104) the reflection for any values of the anchoring coefficient is small and cannot be measured sufficiently accurately. The polar anchoring energy found from Figure 8 is (i) $W = 1.4 \times 10^{-3}$ J m^{-2} for PI 3744, (ii) $W = 0.7 \times 10^{-3}$ J m^{-2} for SD-1 ; (iii) $W = 2.6 \times 10^{-4}$ J m^{-2} for B-15.

We can observe a large variation of LC tilt angle up to 60° for B-15 alignment material. Figure 9 shows the experimental data and the calculated dependence of the LC surface tilt angle on the applied voltage. The best fit for anisotropic coefficients of polar anchoring energy for alignment material B-15 provides the following values: $W_1 = 2.6 \times 10^{-4}$J m^{-2}, $(W_2 - W_1)/W_1 = -0.12$ (Figure 9).

5. Conclusion

A novel method for LC polar anchoring energy measurements based on the measured reflection from an LC cell versus applied voltage is proposed. The 'bulk' electro-optical response of the LC cell was excluded from consideration by a special construction of the LC cell and the geometry of the measurement set-up using 90° twisted LC cell configuration. The high sensitivity of our method guaranties the accurate measurement of the tilt angle on the surface and the LC polar anchoring energy. The results of the polar anchoring energy measurements by the new method are in good agreement with those obtained by a high voltage technique (*10–12*).

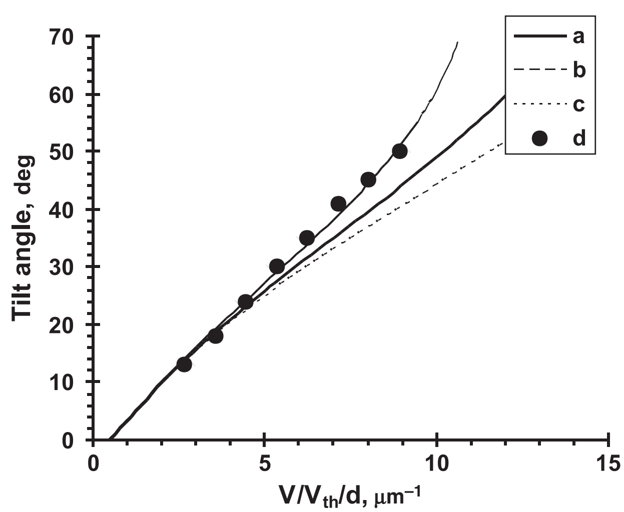

Figure 9. Dependence of the LC surface tilt angle *versus* voltage for various polar anchoring energy coefficients: W_1= 2.6 × 10^{-4} J cm^{-2}; (a) $\Delta W = W_2 - W_1 = 0$; (b) $\Delta W = -0.12 \cdot W_1$, $\Delta W = 0.12 \cdot W_1$; (d) experimental points for the alignment material B-15.

Acknowledgement

This research was supported by HKUST RGC grant 612406, CERG RPC07/08. EG01 and CERG 612208.

References

(1) Chigrinov, V.G. *Liquid Crystal Devices: Physics and Applications*; Artech-House: Boston, MA, 1999.
(2) Blinov, L.M.; Chigrinov, V.G. *Electrooptic Effects in Liquid Crystal Materials*; Springer Verlag: New York, 1994.
(3) Rapini, A.; Papoular, M. *J. Physique* (Paris) **1969**, *Colloq. 30*, C4–(54–56).
(4) Sonin, A.A. *The Surface Physics of Liquid Crystals*; Gordon and Breach: Amsterdam, 1995.
(5) Sugimura, A.; Luckhurst, R.; Zhong-can, O.-Y. *Phys. Rev. E* **1995**, *52*, 681–689.
(6) Hsu, J.-S.; Hsieh, M.-C.; Yang, C.-L.; Liang, B.-J.; Chen, S.-H. *Jpn. J. Appl. Phys.* **2005**, *44*, 6174–6177.
(7) Gu, D.-F.; Uran, S.; Rosenblatt, C. *Liq. Cryst*. **1995**, *19*, 427–431.
(8) Fonseca, J.G.; Galerne, Y. *Phys. Rev. E* **2000**, *61*, 1550–1558.
(9) Subacius, D.; Pergamenshchik, V.M.; Lavrentovich, O.D. *Appl. Phys. Lett.* **1995**, *67*, 214–216.
(10) Yokoyama, H.; van Sprang, H.A. *J. Appl. Phys*. **1985**, *57*, 4520–4526.
(11) Nastishin, Yu. A.; Polak, R.D.; Shiyanovskii, S.V.; Bodnar, V.H.; Lavrentovich, O.D. *J. Appl. Phys.* **1999**, *86*, 4199–4213.
(12) Nastishin, Yu. A.; Polak, R.D.; Shiyanovskii, S.V.; Lavrentovich, O.D. *Appl. Phys. Lett.* **1999**, *75*, 202–204.
(13) Toko, Y.; Akahane, T. *Mol. Cryst. Liq. Cryst. Sci. Technol.* **2001**, *368*, 469–481.
(14) Murauski, A.; Chigrinov, V.; Muravsky, Al.; Yeung, F.S.Y.; Ho, J.; Kwok, H.S. *Phys. Rev. E* **2005**, *71*, 061707.
(15) Yokoyama, H.; Sun, R. *Jpn. J. Appl. Phys.* **2000**, *39*, L45–L47.
(16) Vilfan, M.; Mertelj, A.; Copic, M. *Phys. Rev. E* **2002**, *65*, 041712.
(17) Vilfan, M.; Copic, M. *Phys. Rev. E* **2003**, *68*, 031704.
(18) Hecht, E. *Optics*; 4th ed. Reading, MA: Addison Wesley, 2002.
(19) Mahilny, U.V.; Stankevich, A.I.; Muravsky, A.A.; Murauski, A.A. *J. Phys. D: Appl. Phys.* **2009**, *42*, 075303.